Environmental evaluation of the ULIS PICO1024 microbolometer

Thierry Dartois, Ilias Manolis, Jean-Loup Bézy, Roland Meynart, Christel-Loïc Tisse

Thierry Dartois, Ilias Manolis, Jean-Loup Bézy, Roland Meynart, Christel-Loïc Tisse, "Environmental evaluation of the ULIS PICO1024 microbolometer," Proc. SPIE 10423, Sensors, Systems, and Next-Generation Satellites XXI, 104231L (29 September 2017); doi: 10.1117/12.2279413

SPIE.

Event: SPIE Remote Sensing, 2017, Warsaw, Poland

Environmental evaluation of the ULIS PICO1024 Microbolometer

Thierry Dartois[(1)], Ilias Manolis[(2)], Jean-Loup Bézy[(2)], Roland Meynart[(2)], Christel-loïc Tisse[(3)]*

[(1)]Thales Alenia Space, 5 Allée des Gabians, 06150 Cannes, France
[(2)]European Space Agency, Keplerlaan 1, 2200 AG Noordwijk ZH, The Netherlands
[(3)]ULIS, 364 Route de Valence, Actipole CS 10027, 38113, Veurey Voroize, France

*thierry.dartois@thalesaleniaspace.com

ABSTRACT

In recent years the European Space Agency (ESA) has been pursuing studies dedicated to Earth imaging from space in the Long Wave Infrared region for applications ranging from monitoring of evapotranspiration, and water resources management to the development of urban heat island and monitoring of high temperature events. Among the various solutions being studied is also that of a low cost instrument with moderate needs in terms of resources. .

One potential enabler for such type of mission could be the technology of microbolometer detectors. The latest generation of microbolometer arrays now available offer large formats (XGA) and small pixel sizes which are favourable for keeping the instrument size within reasonable limit while addressing larger swath compared to VGA format. A major concern however, in using commercial microbolometers in space is their ability to sustain the radiation environment of space but also the harsh mechanical environments. COTS microbolometers are potentially susceptible to SEE (single even effects) because of the use of commercial CMOS technology/libraries and no implementation of specific design rules (i.e. space tailored rad hardened). In the past, and in the context of their national program, CNES has performed a space evaluation of COTS microbolometer arrays of 640x480 with 25 µm pitch[3]. Despite successful gamma irradiations and vibration tests; degradation of the ROIC has been evidenced during the heavy ions tests, which makes the full qualification of COTS microbolometers for future space programmes mandatory. Similar tests have been performed on an even earlier device (384x288 with a pitch of 35 µm) under the ESA EarthCARE programme[2].

ESA and Thales Alenia Space have recently run an activity with the objective to validate a third-generation COTS microbolometer offered by ULIS (France) against the relevant environment for a candidate Thermal InfraRed (TIR) space mission. The micro-bolometer selected is the PICO 1024E[1], which offers 1024x768 pixels of size 17 µm square. The validation sequence included the main types of irradiation tests required by a space application as well as vibration and shock tests. Ageing tests are included and synergetic effects are also investigated. The detector performances were tested before, after and during any test sequence. In this paper, the results of this activity achieved in the beginning of 2017 are reported.

Keywords: Microbolometer XGA InfraRed Detector, Space environmental tests, Irradiations, PICO 1024.

1. INTRODUCTION

In the framework of potential future TIR radiometry missions, suitable for the monitoring of Land Surface Temperature on Earth, ESA is currently conducting studies to investigate the feasibility of different instrument concepts and their relevant options as well as breadboarding activities in order to retire any associated technological risks. Among the options being investigated is a small class mission, with moderate radiometric performances based on commercial off-the-self micro-bolometer detectors.

For that reason, Thales Alenia Space has recently conducted a full validation of the PICO 1024 XGA microbolometer from ULIS to verify its capacity to support stringent Space environments with irradiations and mechanical levels covering the need of this type of mission based on small platform generally more demanding than the largest ones.

Sensors, Systems, and Next-Generation Satellites XXI, edited by Steven P. Neeck, Jean-Loup Bézy, Toshiyoshi Kimura, Haruhisa Shimoda, Roland Meynart, Proc. of SPIE Vol. 10423, 104231L
 · doi: 10.1117/12.2279413

The resulting evaluation program worked out by Thales Alenia Space and ESA consisted in environmental stressed tests including heavy ion irradiation, ionizing and non-ionizing irradiation (hence, gamma and protons), Ageing tests, Random vibrations and shocks. The test campaign used several PICO 1024 samples issued without selection from the standard production line of ULIS. This program has been completed by detailed radiometric tests in an economical configuration covering a significant part of the dynamic range.

2. DESCRIPTION OF THE TESTED MICROBOLOMETER

The PICO 1024 is a commercial off-the-self micro-bolometer detectors from ULIS constituted of a 1024 X 768 pixels made from resistive bolometer micro-bridges connected to a silicon readout integrated circuit (ROIC). The sensor is controlled using a serial interface.

The pitch is 17 µm by 17 µm. The device can be operated in 1024 X 768, 640 X 480, 320 X 240 or in user-defined windowing format with the following size constraint: minimum window size of 160 (H) by 80 (V).

Each pixel is equivalent to a thermometer resistance very sensitive to temperature changes. Each resistance is biased by the ROIC, which extracts the resulted current individually for each pixel. A skimming function is in charge of the common mode correction. The resulting current is integrated in a current-voltage conversion stage corresponding to a Capacitance Trans-Impedance Amplifier (CTIA). After signal current-voltage conversion, the bolometer signal is sampled and held and multiplexed to generate the analog video signals. The video signal split over 2 or 4 outputs swings between 0.5 V and 2.9 V.

The detector is row by row readout in a continuous frame rolling shutter mode. While a row of 1024 pixels is being readout, another row is being integrated. The integration time and the integration capacitance (gain) are adjustable.

The PICO 1024 is delivered in a 30 pins-SMT vacuum sealed metallic package, without TE cooler. The optical interface consists of a Germanium window and is compatible with f/1 optics.

Table 1. PICO 1024 main characteristics.

	PICO 1024^{E}	**Remarks**
Format / Pixel pitch	1024 x 768 / 17 µm	
Spectral bandwidth (µm)	8.5 – 17.2 µm	Response > 50 % of max value
Responsivity	8.55 mV/K with Cint=4.3 pF 28.3 mV/K with Cint=1.3 pF	f/1, full spectral band Measured on 6 bolometers
Mean NeΔT	47.8 mK with Cint=4.3 pF	f/1, full spectral band Measured on 6 bolometers
MTF	0.52 along a line 0.6 along a column	Measured at Nyquist Frequency
Max integration time	40.4 µs	
Integration capacitance	1.3 / 2.3 / 4.3 / 5.3 pF	Programmable,
Time constant	12 ms	Not measured in the test campaign
Video output number	2 or 4	Programmable
Power dissipation	260 mW	in 4 outputs mode

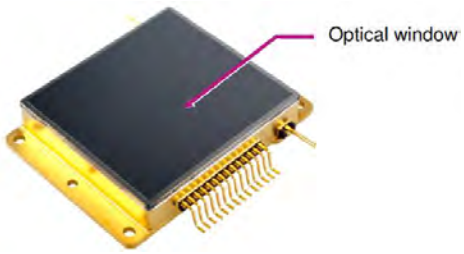

Figure 1. The PICO 1024 is delivered is sealed metallic package without TE cooler.

For the evaluation campaign, 6 standard detectors have been used and characterized by ULIS before delivery and by Thales Alenia Space during initial reference tests. The main radiometric characteristics are given in the Table 2. The slight variance between Responsivity and NeΔT measurements is mainly due to the radiometric accuracy and the noise performance difference between electro-optical test instrumentations used at ULIS and Thales Alenia Space.

Table 2. synthesis of the key radiometric performances issued from the initial Thales Alenia Space (TAS) Reference measurements for the 6 tested micro-bolometers and comparison with ULIS ones in similar conditions (NeΔT and Responsivity only).

	Assumptions	µB1	µB2	µB3	µB4	µB5	µB6
TAS Responsivity (mV)	*4.3 pF/ 38.7 µs*	9.50	9.10	8.90	9.30	9.08	9.09
ULIS Responsivity (mV)	4.3 pF/ 40.4 µs	8.93	8.23	8.30	8.89	8.38	8.47
TAS NeΔT at 301.6 K (mK)	*4.3 pF/ 38.7 µs*	49.5	52.5	55.1	49.3	67.6	52.8
ULIS NeΔT at 300.6 K (mK)	4.3 pF/ 40.4 µs	45.2	49.1	49.6	44.5	49.7	48.8
Temporal noise (µV)	4.3 pF/ *38.7* µs	464	472	488	456	565	475
Operability: Number of defective pixels	Resp at 4.3 pF	130	167	161	288	284	171
	NeDT at 4.3 pF	17	76	77	34	135	83
PRNU (%)	Best case at 2.3 pF (f/1)	0.16	0.27	0.24	0.32	0.3	0.34

3. TEST SEQUENCE DESCRIPTION

The evaluation program includes the following activities (see Figure 2):

- Heavy ions tests (Single Event Latchup: SEL) on 3 open microbolometers (window removed),
- Detailed radiometric tests on 2 standard microbolometers to evaluate radiometric performances as responsivity, PRNU, temporal and spatial noises, NeΔT and linearity.
- Ageing tests at hot temperature and Total Ionizing Dose (TID) tests on 3 standard microbolometers,
- Vibrations on 2 standard microbolometers followed by shocks on one microbolometer,
- Total Non-Ionizing Dose (TNID: protons) tests on 3 standard microbolometers.
- Detailed radiometric tests on one standard microbolometer after the complete stress sequence.

For each test using standard microbolometer, a reference detector has been added to follow the evolution of the test bench. For irradiations (TID), ageing tests, heavy ions and protons tests (TNID), 3 devices have been stressed to improve the credibility of the result without entering in a full qualification process, which was not the goal of this evaluation.

The distribution of the 9 available devices is provided in the Figure 2. Two detectors (µB2 and µB3) have been submitted to synergetic stress: ageing, TID, vibrations and shocks (µB3 only).

Before and after each stress step, a reference radiometric test consisting in acquisitions at 2 radiances had been performed. From this repetitive test, Current consumption, Responsivity, NeΔT, PRNU and Offset have been derived and followed-up.

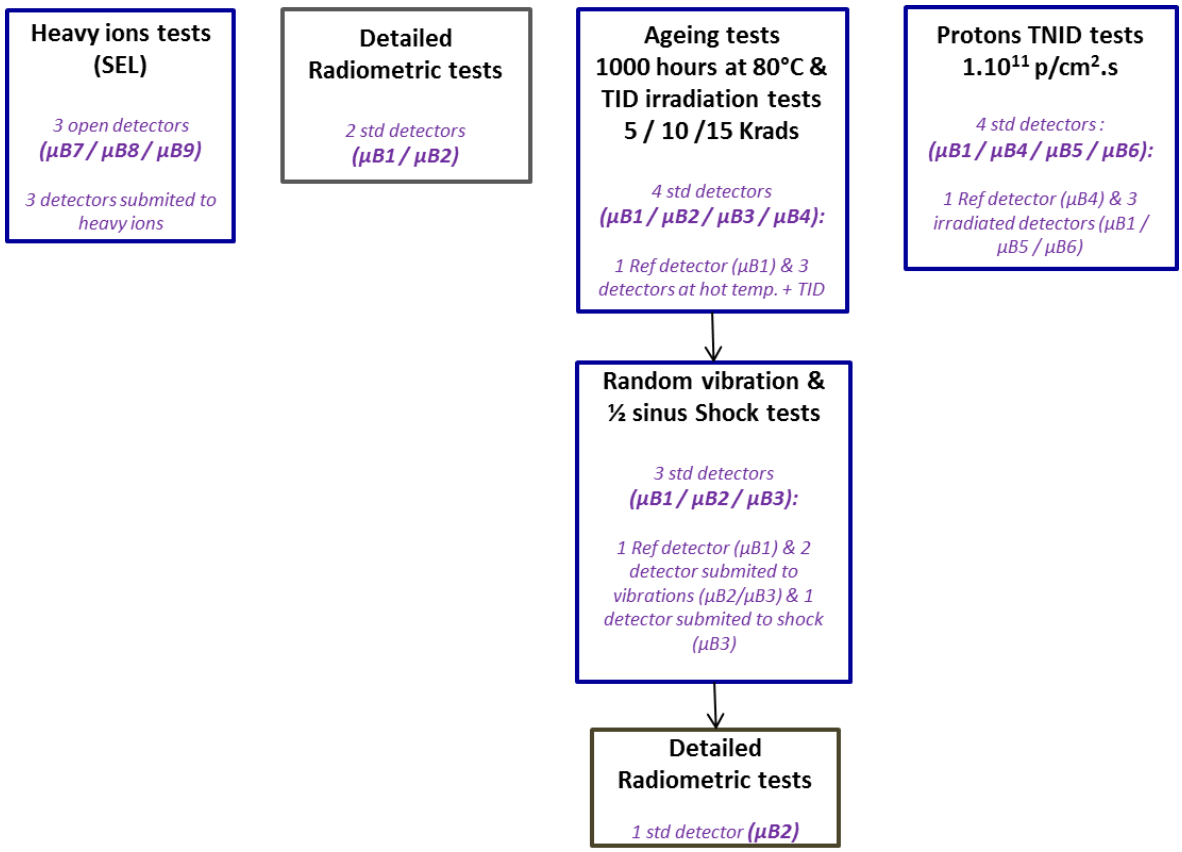

Figure 2. PICO 1024 microbolometer evaluation program applied on 9 detectors.

4. HEAVY IONS TEST RESULTS

The heavy ions tests performed on 3 open microbolometers have been done for LET between 3.3 and 62.5 MeV.cm2/mg with a fluence of 1.10^7 equivalent protons/cm^2 (used for all the runs). The tests have been done in nominal supply conditions and for a nominal frame rate of 30 Hz.

There is no latch-up on VDDA and VDDL on the 3 tested detectors for LET between 3.2 and 62.5 MeV.cm2/mg. This good behavior has been confirmed also with an extended frame rate of 50 Hz.

Video signal shape changes starting at 3.3 MeV.cm2/mg and confirmed by random current consumption variations on VDDA/VDDL/VBUS and VSK have been observed. These changes were observed during all irradiation runs and for all tested detectors with an apparition rate increasing with the ions LET increase. These events are likely due to SEUs in the SERDAT register of the device that induced an unknown programming state of the detector.

The conclusion of the Heavy ions test campaign was that the PICO 1024 is not sensitive to SEL, but it seems to be subject to SEU which can be compensated by frequent programming of the serial register.

5. AGEING AND TID TESTS RESULTS

5.1 Ageing tests results

The current consumptions of the 6 biases/supplies (VDDA, VDDL, GFID, GSK, VSK+GOC, VBUS) followed on the 3 tested microbolometers during the 1000 hours at 80°C have not evolved.

There is also no evolution outside the criteria of the radiometric parameters after the Ageing tests

5.2 TID tests results

There is no current evolution on the six power supplies and biases (GFID, GSK, VBUS, VDDA, VDDL and VSK/GOC) after the TID test sequence applied in 3 steps (5.7 / 10.9 /15.6 Krads) and followed by an annealing phase of 576 hours at 80°C. This demonstrated the good reliability of the PICO 1024 which could sustain an orbital life of 8 years at 30 °C (equivalent to 1576 hours at 80 °C).

The Responsivity is globally not affected by the TID tests : the criteria (evolution < ± 5 %) has been respected with a margin higher than a factor of 2.

The PRNU is globally constant with some slight variations, fully recovered after a long annealing at 80°C.

The NeΔT criteria (evolution < ± 7 %) has been globally met, with some incidental variations due to temporal noise evolutions explained by (i) a degraded grounding configuration and (ii) a non-optimized video signal sampling position (not programmable in the system used for the test). A mean NeΔT increase of 2.5 % (largely lower than the criteria) has been observed after the first annealing of 24 hours. Here again, it has been recovered after the long annealing at 80°C.

The parameter which has the most evolved is the offset, with a lot of values higher than the success criteria of ± 5 % or of the absolute criteria of ± 20 mV. For all detectors, the offset amplitude decreases with the dose level with a low recovery after the first annealing and a stronger one after the second annealing at 80 °C. The results illustrated by the Figure 5 show a mean offset reduction of about -40 mV at Cint=2.3 pF, with a worst case at -51 mV for µB3 and about -30 mV at Cint=4.3 pF with a worst case at -41 mV for µB3. It has been concluded that the dose level induces an offset reduction which is low in regard to the PICO 1024 dynamic range (2.4 V). Moreover, this evolution is almost recovered after a long annealing at 80°C with a mean final difference of only -17 mV.

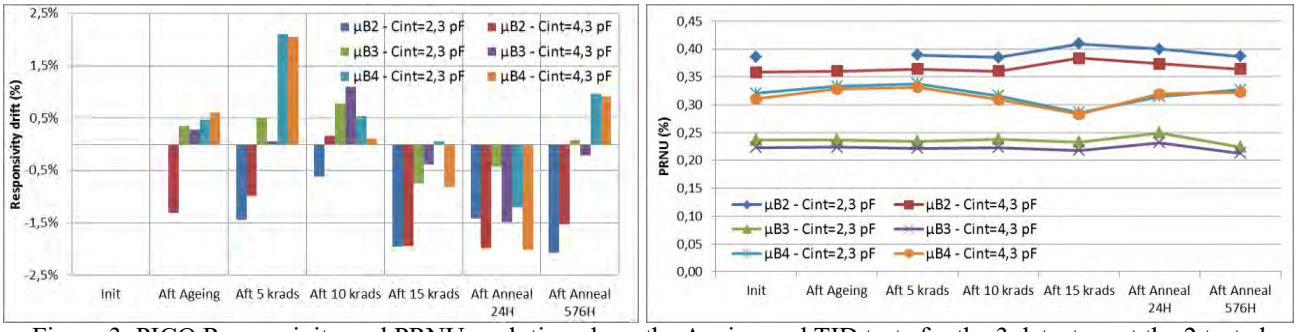

Figure 3. PICO Responsivity and PRNU evolution along the Ageing and TID tests for the 3 detectors at the 2 tested gains. The statistical tendency is a slight reduction of the responsivity, but largely lower than the measurement accuracy. After the final annealing of 576 hours at 80 °C, the main PRNU evolutions have been recovered.

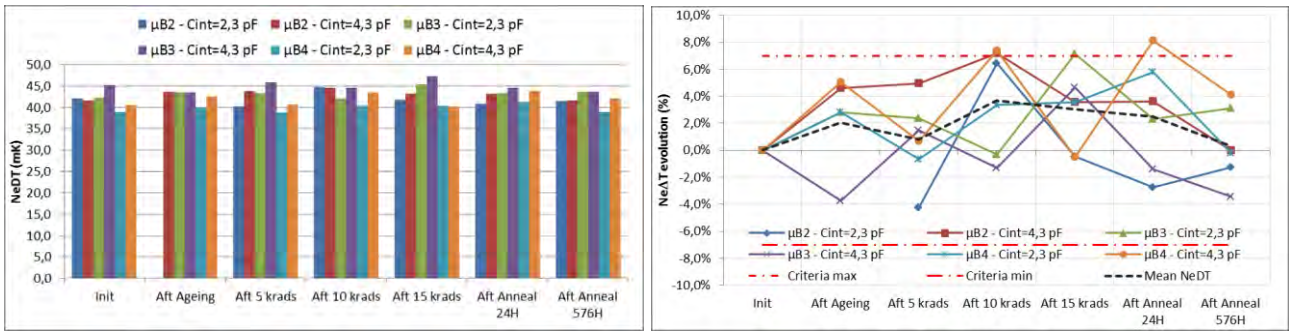

Figure 4. NeΔT evolution along the Ageing and TID tests for the 3 detectors at the 2 tested gain. The tendency is a mean NeΔT degradation of 2.5 % after the first annealing of 24 hours and a full recovery after the long annealing at 80°C.

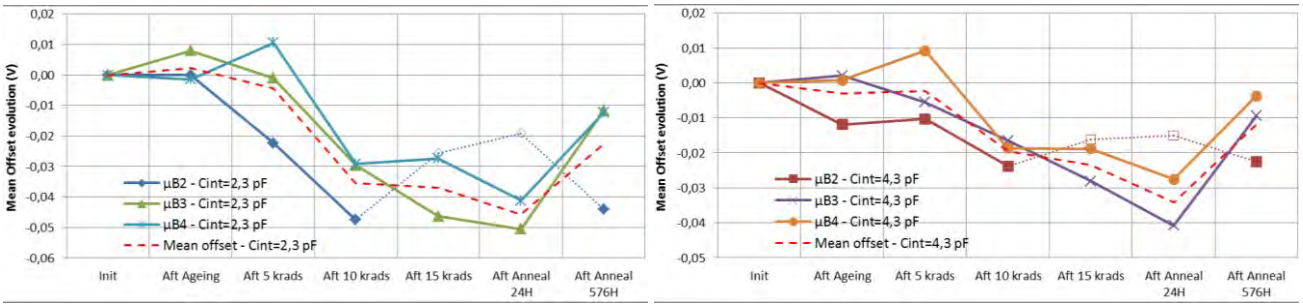

Figure 5. Mean offset evolution along the Ageing and TID tests for the 3 detectors at the 2 tested gains after correction of the detector temperature variations during the test. The tendency is a low reduction with the dose level especially for the highest gain and a good recovery for µB3 and µB4 after the annealing at 80°C. For µB2, the points after 15 Krads and after annealing of 24 hours have an atypical behaviour due to limitation of the offset correction method, then not used for the mean offset calculation.

6. RANDOM VIBRATIONS AND SHOCK TESTS RESULTS

The PICO 1024E has been initially qualified for military and defense applications in accordance with MIL-STD-810 and MIL-STD-883 military test standards. The PICO 1024E successfully passed all required random vibration, sinusoidal vibration and shocks test.

In the present evaluation for space applications, random vibrations and shock testing with 5.5 times more stringent levels in average than MIL-STD-810 and MIL-STD-883 have been applied to 2 standard detectors after being stressed by irradiations (TID) and ageing tests, as detailed in Figure 6.

The defective pixel rate for the PICO 1024E is typically less than 0.1%: an initial amount of 174 defective pixels was observed for the first detector (µB2) at delivery time by ULIS. After the vibration step along the Z-axis, the operability of this first detector (µB2) was non-negligibly degraded with the apparition of a few thousands of additional non-operating pixels mostly concentrated onto 12 columns of the focal-plane-array, and more marginally scattered in a random manner on the array by clusters of 2-3 pixels. After the X axis vibrations, the amount of non-operating pixels had increased again to reach a defective rate slightly over 1%. A similar degradation was not confirmed on the second detector (µB3) despite the following shock test campaign. This second observation demonstrates the robustness capability of the PICO1024E to withstand vibration and shocks up to 35g RMS and 2000g srs, respectively.

A structural failure analysis of the detector µB2 was performed at ULIS to identify and correct the root cause for mass production. For instance, numerous extra cleaning and post-vacuum sealing steps were implemented throughout the assembly process to remove or immobilize all loose particles of sufficient mass that could be present in the cavity of the metallic package and, upon impact with the blind or active pixels, cause damage or breakage of their bolometric membranes.

The other parameters (power consumption, NeΔT, PRNU, NeΔT & offset) have not evolved after vibrations and shocks.

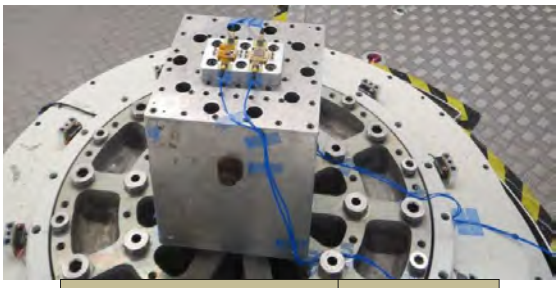

Random frequency	Level
20 – 100 Hz	3 dB/oct
100 – 800 Hz	1 g^2/Hz
800 – 2000 Hz	-6 dB/oct
Overall	35 g RMS

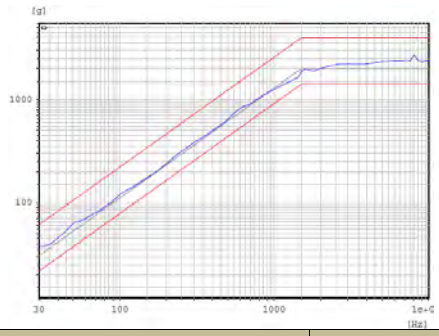

Random frequency	Level
20 Hz	20 g srs
1500 Hz	2000 g srs
10000 Hz	2000 g srs

Figure 6. Random vibrations levels applied on X and Z axis and shock levels applied on Z axis only. After the random vibrations, one detector has been submitted to shock tests on one axis.

7. TNID (PROTONS) TEST RESULTS

Protons irradiations at a fluence of 1.10^{11} p/cm^2 with protons of 50.8 MeV have been applied on 3 unbiased detectors.

After irradiations there is no evolution of the individual currents of the six power supplies and biases (GFID, GSK, VBUS, VDDA, VDDL and VSK/GOC) controlled before and after protons irradiations.

The radiometric key parameters (NeΔT, PRNU, NeΔT & offset) issued from the reference radiometric tests performed before and after the protons irradiations have not evolved after the TNID tests. The continuous biasing of 24 hours doesn't change the values of these key parameters.

8. RESULTS OF DETAILED RADIOMETRIC TESTS BEFORE AND AFTER THE STRESS SEQUENCE

8.1 Sensitivity to integration time (TINT)

The responsivity increases linearly with the integration time which is not the case of the video signal level. This is due to the input stage architecture of the ULIS detector which justifies the output signal level provided by the following simplified expression:

$V_{OUT} = V_{BUS} - \frac{T_{\text{int}}}{C_{\text{int}}}.(\frac{Upol_{blind}}{R_{blind}} - \frac{Upol_{pix}}{R_{pix}})$, where Rblind and Rpix which are respectively the blind and active pixel resistances depend of the integration time (Tint) due to self heating.

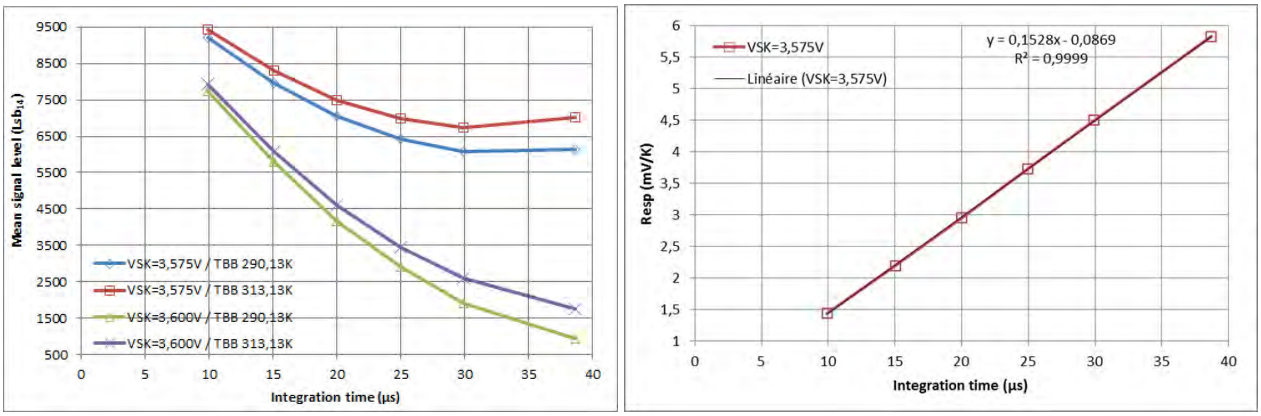

Figure 7. µB1 output signal (left curve) as a function of integration time for 2 black body temperatures and at 2 VSK values. The curve on the right shows that the responsivity as a function of integration time is perfectly linear.

8.2 Sensitivity to active bolometer bias (GFID)

The main radiometric performances (especially the NeΔT) are slightly dependent of the active bolometer bias level. A low NeΔT improvement of 8.4 % for µB1 and 5.5 % for µB2 has been demonstrated with an increase of GFID from 2.8 V (ULIS recommended value) to 2.84 V (best compromise between all parameters). The stress sequence applied on µB2 has not affected these results.

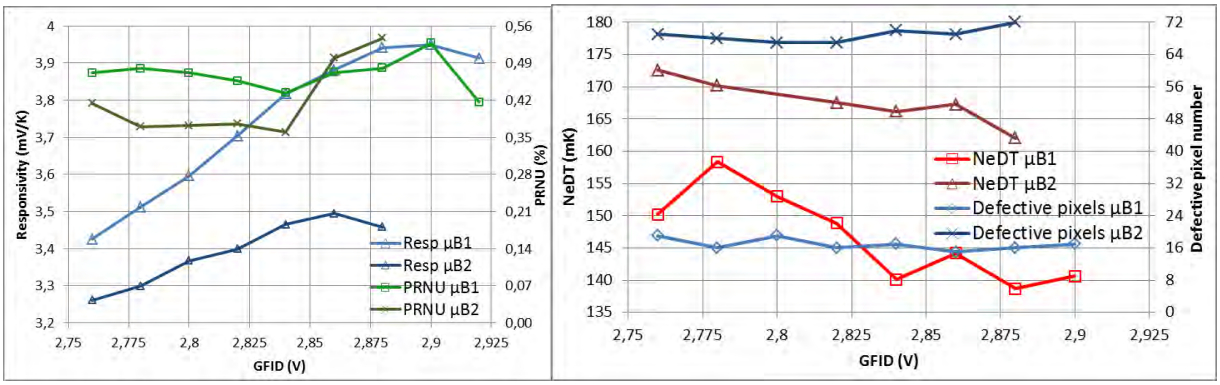

Figure 8. Responsivity, PRNU and NeΔT as a function of GFID for 2 tested detectors (µB1 and µB2).

8.3 Linearity measurements results

The Figure 9 and Figure 10 provide the results of the linearity measurements performed on µB1 (only before stress) and on µB2 (before and after stress) at f/1 in an extended black body temperature range, generally between -15 and +80°C. The best demonstrated integral non linearity (p-p NL) are:

- 1 % for µB2 in a dynamic range of 1.06 V with Cint=1.3 pF,
- 1.29 % for µB1 in a dynamic range of 1.6 V with Cint=2.3 pF.

The non linearity curves measured after stress on detector µB2: have the same shape than the initial ones. Some degradations of the peak to peak non linearity have been observed but generally lower than ± 0.5 % (only one case with the highest tested dynamic range: f/1, Cint=1.3 pF is higher with NLp-p difference of 0.7 %). Then, it has been concluded that the non linearity is only slightly affected by the stress (most parts of the degradation came from the use of a simplified radiometric test configuration).

The differential non linearity or spatial noise calculated on the full frame and provided in the Figure11 is low compared to the temporal noise (between 3 to 6,4 times lower) also reported in the same figure.

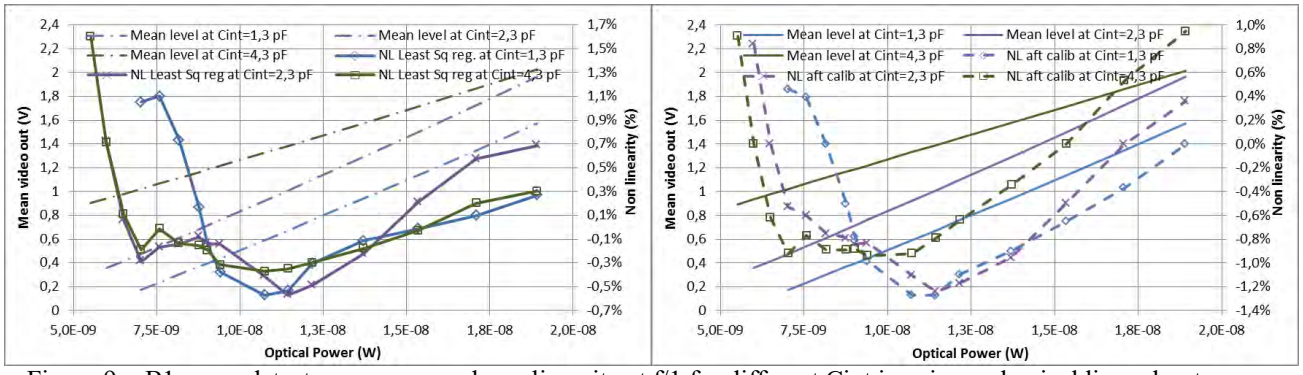

Figure 9. µB1 mean detector response and non linearity at f/1 for different Cint in using a classical linear least square regression on the left curves and after linear calibration in 2 fluxes on the right curves.

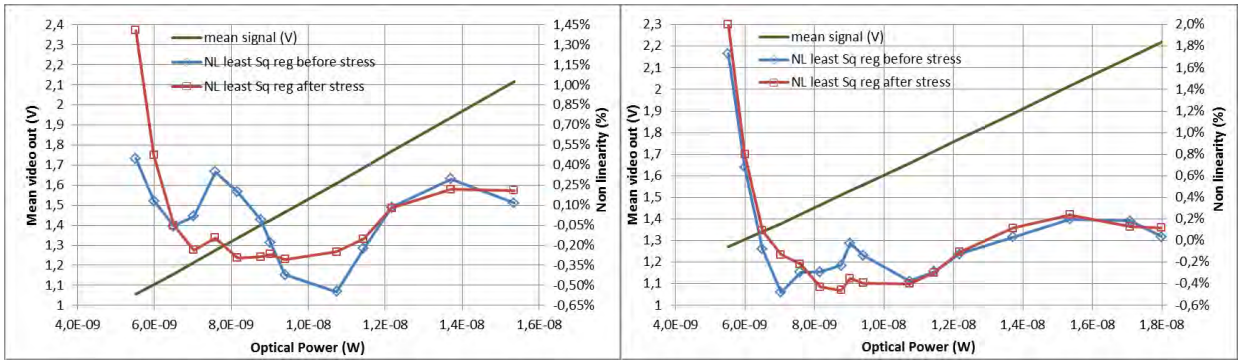

Figure 10. µB2 mean detector response and non linearity before and after stress at f/1 for Cint=1.3 pF (left curve) and Cint=4.3 pF (right curve).

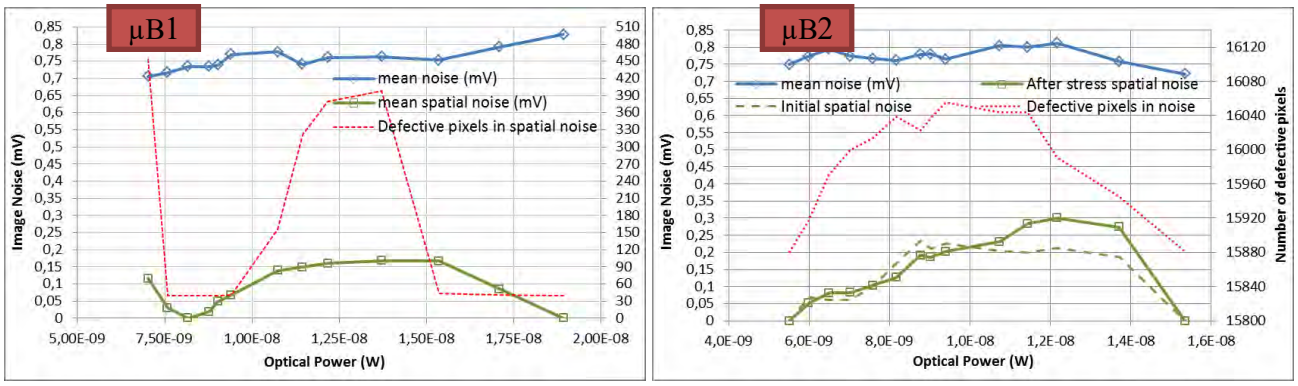

Figure 11. mean temporal and spatial noises at f/1 with Cint=1.3 pF for the 2 tested detectors. The image (low frequency) spatial noise is calculated with a linear calibration at 2 fluxes. For µB2 the curve shows that except the number of defective pixels, the spatial noise is not affected by the synergetic effect.

The main radiometric performances (Responsivity and noises) measured on µB2 summarized in the Table 4 have not evolved after application of the complete stress test sequence. The degradation of spatial noise is only due to the loss of pixels due to random vibrations.

Table 3. Synthesis of linearity measurements for the 2 tested detectors. The results have been obtained with the classical linear least square regression. The mean values correspond to averages of the NL processed at the different fluxes

Parameters	Assumptions	µB1 Initial	µB2 Initial	µB2 After stress
NL with LMS method p-p value in %	*f/1 - 1.3 pF/ 18.1 µs*	**1.67 %**	**1.00 %**	**1.71 %**
	f/1 - 2.3 pF/ 32 µs (µB1) 18.1 µs (µB2)	**1.29 %**	**1.7 %**	**NM**
	f/1 - 4.3 pF/ 38.7 µs	**1.97 %**	**2.21 %**	**2.46 %**
NL with LMS method mean value in %	*f/1 - 1.3 pF/ 18.1 µs*	**0.42 %**	**0.22 %**	**0.31 %**
	f/1 - 2.3 pF/ 32 µs (µB1) 18.1 µs (µB2)	**0.33 %**	**0.26 %**	**NM**
	f/1 - 4.3 pF/ 38.7 µs	**0.32 %**	**0.32 %**	**0.39 %**

As a general conclusion of the synergetic effects, it can be stated that the mean characteristics of µB2 have evolved only marginally after the complete stress sequence (shocks not applied on µB2) and that the strong degradation of the operability of this detector after vibrations cumulated with the accuracy of the test bench are probably at the origin of these slight degradations of noise and linearity.

Table 4. synthesis of the main radiometric performances measured before and after the stress tests on µB2

Parameters	Assumptions	Initial	After stress
Mean Responsivity (mV)	*f/1 - 1.3 pF/ 18.1 µs*	14.9	14.7
	f/1 - 4.3 pF/ 38.7 µs	10.8	10.8
Mean temporal noise (mV)	*f/1 - 1.3 pF/ 18.1 µs*	0.753	0.774
	f/1 - 4.3 pF/ 38.7 µs	0.472	0.482
Mean Spatial noise (Avg of all acquisitions)	*f/1 - 1.3 pF/ 18.1 µs*	162 µV	176 µV
	f/1 - 4.3 pF/ 38.7 µs	117 µV	166 µV
Mean NeΔT (mK)	*f/1 - 1.3 pF/ 18.1 µs*	47.6	48.5
	f/1 - 4.3 pF/ 38.7 µs	45.3	46.3

9. CONCLUSIONS

The 2nd generation version of the PICO 1024E has proven its capability to support space environments. It is not sensitive to Single Event Latchup (SEL) up to 62.5 MeV.cm^2/mg. This is a strong improvement compared to the previous VGA format ULIS microbolometer which was sensitive to SEL.

Nevertheless, the PICO 1024E seems to be sensitive to SEU, from 3,3 MeV.cm2/mg, which however is not seen as a showstopper as it can be tackled in reality by frequent re-programming during operations.

The ageing tests (1576 hours at 80°C) and the gamma irradiations (TID) applied on 3 devices (with a level of 15,6 Krads) have not modified the electrical interfaces current consumptions and not degraded the responsivity nor the NeΔT. Nevertheless, a mean offset reduction of -50 mV has been observed after 15.6 Krads, which has been partially recovered with a long annealing at 80°C (-17 mV remaining). Compared to the detector dynamic range of 2.4 V, this offset evolution is negligible. The PICO 1024E is also not sensitive to 50 MeV protons environment up to 1.10^{11} p.cm^2.

The detector and the technologies used are robust and can support stringent random vibrations (35 grms) and shocks levels (2000 g between 1500 - 10000 Hz). In addition to the precaution steps implemented by ULIS during the assembly process to eliminate the risk of loose particles inside the vacuum package, a dedicated non-destructive screening could be recommended for space applications.

From the detailed radiometric measurements it can be concluded that:

- The Integral Non Linearity (p-p) is around 1.3 % on a dynamic range of about 1.6 V.
- The synergetic stress has not induced degradation of the main radiometric performances.
- The PRNU is low, generally lower than 0.34 %, but can be as low as 0.16 % for an excellent detector.
- The spatial noise is low compared to the temporal noise: 3 to 9 times lower.

REFERENCES

[1] C. Trouilleau, B. Fièque, S. Noblet, F. Giner, D. Pochic, A. Durand, P. Robert, S. Cortial, M. Vilain, J.L. Tissot, and J.J. Yon, "High-performance uncooled amorphous silicon TEC less XGA IRFPA with 17µm pixel-pitch," Proceedings of SPIE 7298, (2009)

[2] G. Hopkinson, L. Gomez Rojas, M. Skipper and R. Meynart, "Testing of InGaAs, microbolometer and pyroelectric detectors in support of the EarthCARE mission," Proceedings of SPIE 7106 (2008)

[3] H. Geoffray, G. Quadri , L. Tauziède, A. Materne , A. Bardoux, "Evaluation of a COTS microbolometers FPA to space environments," Proceedings of SPIE 7826 (2010)

ACKNOWLEDGEMENTS

This activity was funded by the European Space Agency under the contract No. 4000116620/16/NL/FF/gp. Thales Alenia Space and ESA would like to thank ULIS for their collaborative approach and help in the interpretations of the behaviour of the PICO 1024 under the different stresses.